RESEARCH ARTICLE

Directional Variability of the Isometric Force Vector Produced by the Human Hand in Multijoint Planar Tasks

Jason Friedman[1,2], Mark L. Latash[2], Vladimir M. Zatsiorsky[2]

[1]ARC Centre of Excellence in Cognition and its Disorders, Macquarie University, Sydney, Australia. [2]Department of Kinesiology, The Pennsylvania State University, University Park.

ABSTRACT. Numerous studies have examined control of force magnitude, but relatively little research has considered force direction control. The subjects applied isometric forces to a handle and the authors compared within-trial variability when force is produced in different directions. The standard deviation of the force parallel to the prescribed direction of force production increased linearly with the targeted force level, as did the standard deviation of the force perpendicular to the instructed direction. In contrast, the standard deviation of the angle of force production decreased with increased force level. In the 4 (of 8) instructed force directions where the endpoint force was generated due to a joint torque in only 1 joint (either the shoulder or elbow) the principal component axes in force space were well aligned with the prescribed direction of force production. In the other directions, the variance was approximately equal along the 2 force axes. The variance explained by the first principal component was significantly larger in torque space compared to the force space, and mostly corresponded to positive correlation between the joint torques. Such coordinated changes suggest that the torque variability was mainly due to the variability of the common drive to the muscles serving 2 joints, although this statement needs to be supported by direct studies of muscle activation in the future.

Keywords: direction, isometric force, torque, variability

The control of force magnitude has been studied in depth (reviewed in Carlton & Newell, 1993). In a study of rapid, uncorrected isometric unidimensional force production to a target (sometimes termed *impulse force*), it was observed that the standard deviation of the force magnitude at the target, across trials, increased approximately linearly with the magnitude of the target force (Schmidt, Zelaznik, Hawkins, Frank, & Quinn, 1979). This finding has been replicated in studies using constant visual feedback gain (Hamilton, Jones, & Wolpert, 2004; Slifkin & Newell, 1999)—for example, 1 cm on the screen equals the same force for all levels of target force production—and scaled feedback (Shapkova, Shapkova, Goodman, Zatsiorsky, & Latash, 2008; Tracy, Mehoudar, & Ortega, 2006), where 1 cm equals a fixed proportion of the target force. The variability has been observed to level off at about 65% of maximal force and then decrease at higher levels (Sherwood & Schmidt, 1980). Later studies suggested that the force magnitude variability is also dependent on the time to produce the peak force, rather than force magnitude only (Hong, Lee, & Newell, 2007; Newell & Carlton, 1988; Slifkin & Newell, 2000).

In contrast, there are fewer studies on the variability of force direction. These studies can be classified into two gro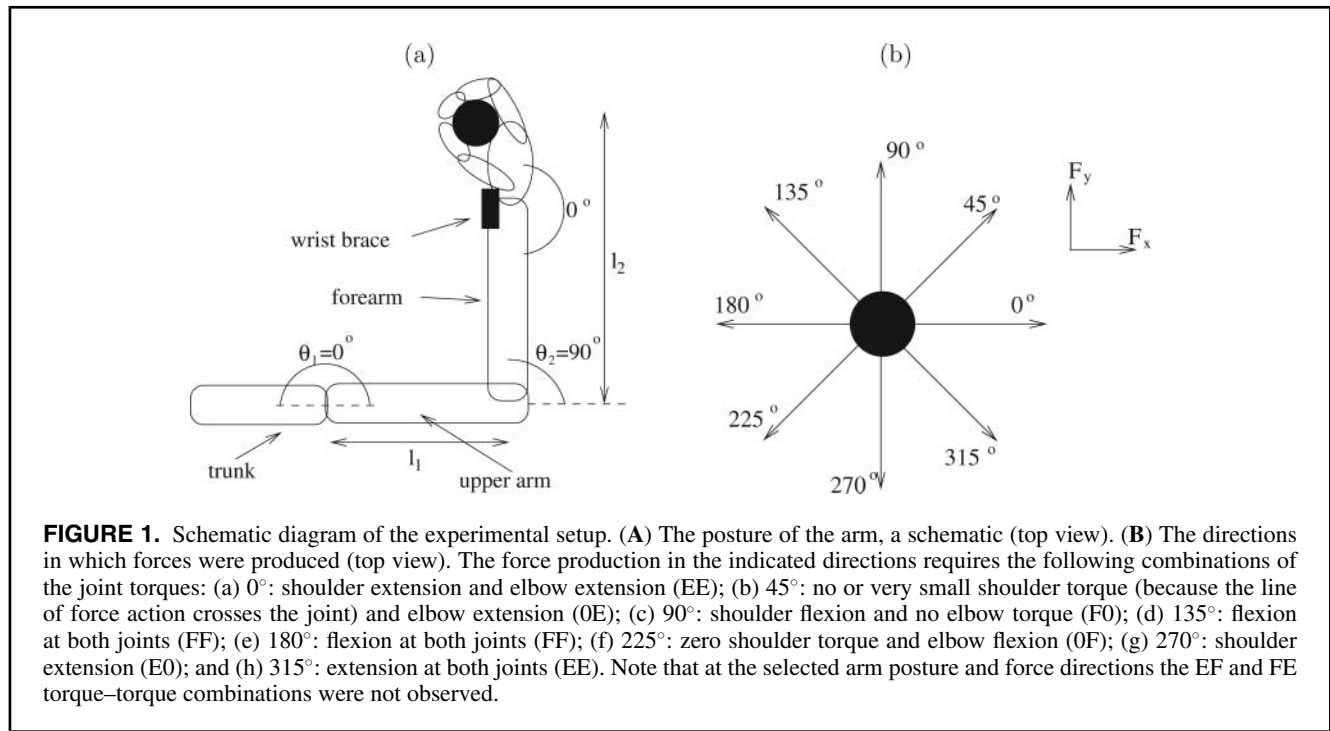ups that deal with exploring the force production in (a) single 2- or 3-D joints (e.g., Kutch, Kuo, Bloch, & Rymer, 2008) or (b) in planar kinematic chains. Due to evident reasons, these tasks are biomechanically quite different.

Kutch et al. (2008), studying the endpoint force during isometric force production of the index finger metacarpophalangeal joint in different directions found that fluctuations in the covariance of force projections on the coordinate axes were dependent on whether the direction of force production was close to the direction of muscle action of one of the muscles involved. From this finding, they inferred that muscles are recruited flexibly and not according to fixed groupings.

Studies on the effect of the force direction on the force variability in multilink tasks have been mainly limited to fingertip force production in the flexion–extension plane. It was observed that the target direction significantly affected the variable error of the force direction, but not the constant error (Gao, Latash, & Zatsiorsky, 2005). Force direction variability was shown to be larger in one-finger tasks as compared with four-finger tasks and larger for force production downward and toward the body as compared with other directions (Kapur, Friedman, Zatsiorsky, & Latash, 2010). Valero-Cuevas, Venkadesan, and Todorov (2009) examined muscle coordination using electromyograms during fingertip isometric force production and found that the variance is consistently lower in task-revelant parameters than at the muscle level.

There is not a clear consensus about the source of variation observed in force production, although it is generally assumed to reflect neuromotor noise (reviewed in Newell, Deutsch, Sosnoff, & Mayer-Kress, 2006). It has been assumed that the amount of noise increases with the neural signal, the phenomenon known as signal-dependent noise (Harris & Wolpert, 1998). Jones, Hamilton, and Wolpert (2002) concluded that the signal-dependent noise is mostly related to neural sources. In an experiment involving extension of the distal phalange of the thumb, they found that when the same muscles were electrically stimulated, the variation (noise) did not increase with the force level. Peripheral sources may also contribute to the variability of the motor output, and attempts have been made to distinguish between these two sources (Wing & Kristofferson, 1973).

Correspondence address: Jason Friedman, ARC Centre of Excellence in Cognition and its Disorders, C5C Level 4, Macquarie University, Sydney, NSW 2109, Australia. e-mail: jason.friedman@mq.edu.au

FIGURE 1. Schematic diagram of the experimental setup. (**A**) The posture of the arm, a schematic (top view). (**B**) The directions in which forces were produced (top view). The force production in the indicated directions requires the following combinations of the joint torques: (a) 0°: shoulder extension and elbow extension (EE); (b) 45°: no or very small shoulder torque (because the line of force action crosses the joint) and elbow extension (0E); (c) 90°: shoulder flexion and no elbow torque (F0); (d) 135°: flexion at both joints (FF); (e) 180°: flexion at both joints (FF); (f) 225°: zero shoulder torque and elbow flexion (0F); (g) 270°: shoulder extension (E0); and (h) 315°: extension at both joints (EE). Note that at the selected arm posture and force directions the EF and FE torque–torque combinations were not observed.

In this work, we were specifically interested in (a) the variability of the endpoint force, its magnitude and direction, as a function of the target force magnitude and direction; and (b) the torque variability at the contributing joints, the shoulder (τ_1) and elbow (τ_2) torques. To do that, we asked subjects to generate a targeted force in instructed directions (Figure 1). We intentionally examined a relatively simple system. We restricted the right arm to lie in a horizontal plane at the height of the shoulder, with the upper arm in the frontal plane, and the elbow flexed at 90° (see Figure 1A). By securing the shoulder to the chair, and bracing the wrist, we had a system with two degrees of freedom to produce two-dimensional forces. This allowed us to reconstruct the τ_1 and τ_2 variability from the recorded endpoint force variability (explained subsequently). In contrast to most of the studies described previously, and due to the large number of conditions (32), we considered variation within a trial, not across repetitions.

Our interest in the joint torque variability was motivated by the following reasoning. A natural sequence of events in the endpoint force production is from the muscle forces to the endpoint force: muscle forces → joint torques → endpoint force. In this sequence, the joint torques are a cause of the endpoint force, and hence the endpoint force variations are due to the joint torque variability. Changes in the endpoint force magnitude without changing the endpoint force direction require synchronous and proportional changes of the joint torques (explained in Chapter 2 in Zatsiorsky, 2002). For example, if the joint torque magnitudes double the endpoint force magnitude also increases by a factor of two while its direction does not change. All other joint torque variations—synchronous but not proportional changes when joint torques vary by different factors, say 1.1 and 1.5, as well as asynchronous torque variations—result in changes in force direction. Exploring the joint torques variation, in particular the torque–torque correlation, may help in understanding the causes and mechanisms of the endpoint force variability.

We proposed five hypotheses. Note that values in italics are scalars and values in bold are vectors. First, we expected that due to the relatively low forces (≤40% maximal force [MVC]), the standard deviation of the force magnitude |F| would increase linearly with the instructed force level, F_i, as has been found in numerous other studies (Schmidt et al., 1979; Shapkova et al., 2008; Vaillancourt & Newell, 2003). Second, we similarly expected that the standard deviation of the force perpendicular to the prescribed direction of force production, $F_\perp$, would increase linearly with the required force vector magnitude, as was found in Kapur et al. (2010). Third, we expected that the standard deviation of the angle of force production would increase with the force magnitude (i.e., the larger the force the less precise is the force direction). A fourth hypothesis was that that the axes of the principal components of the force–force distributions (using principal components analysis) would be aligned with the average direction of produced force, $\mathbf{F}_\parallel$, and the direction perpendicular to the average direction, $\mathbf{F}_\perp$. This would occur if force production is produced with little covariation between |F| and $F_\perp$ (i.e., between the magnitude of the produced force and the magnitude of the force component perpendicular to the average direction of the previous force). Following

the first three hypotheses, we expected that the joint torque variability would increase with the torque magnitude (the fifth hypothesis). Due to the novelty of the research, we did not formulate specific hypotheses about (a) the dependence of the joint torque variability on the endpoint direction and (b) the effect of the endpoint force magnitude and direction on the concomitant torque–torque variations (e.g., on the torque–torque correlations in the trials). This part of the research can be regarded as exploratory.

Method

Subjects

Four male and four female right-hand-dominant subjects took part in this study (M age $= 25.5 \pm 4.1$ years; M weight $= 62.6 \pm 10.9$ kg; M height $= 1.68 \pm 0.07$ m; shoulder to elbow (upper arm) length $= 28.2 \pm 1.4$ cm; elbow to center of handle length $= 32.1 \pm 2.0$ cm). All subjects were healthy, with no known neurological or peripheral disorders. All of the subjects gave informed consent according to the policies of the Office for Research Protections at the Pennsylvania State University.

Apparatus

The apparatus is shown in Figure 2. An aluminum cylindrical handle (height 15 cm, diameter 2.5 cm) was attached to a 3-DOF force sensor (model 9347C, Kistler Instruments AG, Winterthur, Switzerland). The force sensor was mounted on an aluminum block, which could slide left and right along

two poles. These two poles were attached to blocks on the left and right side of the apparatus, which could slide forward and back on another two poles. Screws on the central block, and on the two side blocks permitted fixing the handle at a desired location. The total workspace was 65×65 cm.

The subject sat on a large, heavy chair, and was strapped to the chair with two seatbelts to prevent movement of the trunk. The chair sat on a hydraulic lift, and its height was adjusted for each subject such that the bottom of the handle was at shoulder height. The forearm was supported by a padded semicircular piece of plastic pipe, hanging down directly vertically from the ceiling. The location of the handle was adjusted for each subject such that the upper arm was parallel to the coronal plane and the elbow was flexed such that there was a $90°$ angle between the upper arm and forearm (see Figure 1A). The selected chair height ensured that the upper arm and forearm lay in a horizontal plane, at the height of the shoulder. A wrist brace was used to prevent rotations at the wrist. The subjects grasped the handle with a power grip (i.e., they wrapped their fingers tightly around the handle).

Experimental Procedure

The subjects were provided with feedback on the horizontal components of the force vector produced on the handle by the right arm using a monitor placed directly in front of them. A blue arrow showed the amount and direction of force they were generating. They were shown three concentric circles, subdivided into eight directions, which filled the screen. Initially, the subjects were asked to produce MVC for
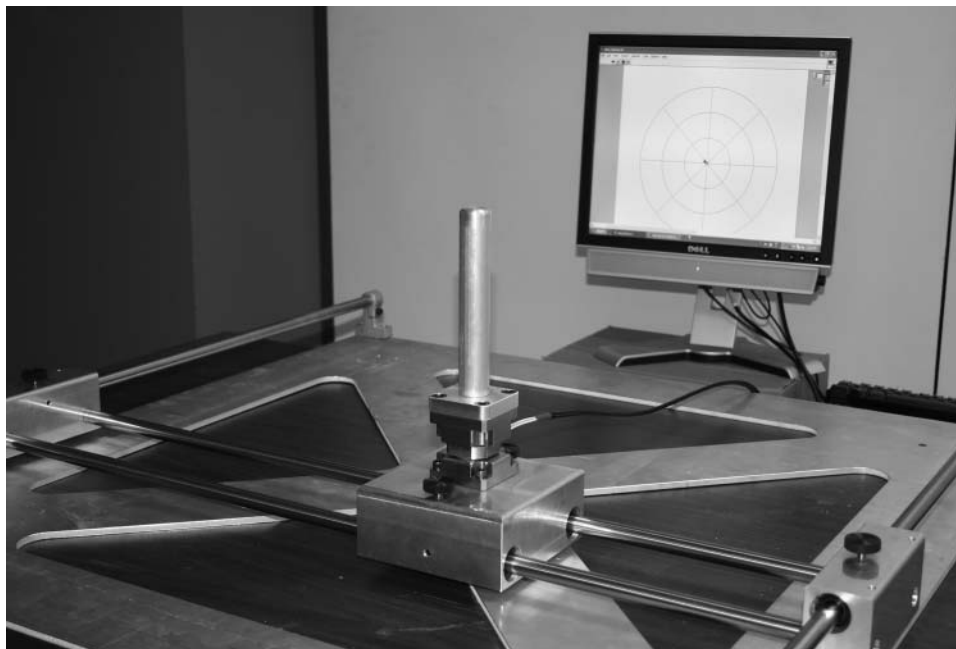

FIGURE 2. Experimental setup.

5 s along each of the eight directions, in a random order. Each MVC recording was performed twice, and the highest force produced during either of these recordings was used to set the relative force levels and in the subsequent analysis.

For the remainder of the experiment, four equally spaced concentric circles were shown, and the feedback was scaled for each trial such that each circle corresponded to a multiple of 10% of MVC for the appropriate direction (i.e., the outermost circle corresponded to 40% MVC). In each trial, the subject was required to produce force at 5%, 10%, 20%, or 40% of MVC. The target force level and direction (one of the eight directions) was indicated by a red cross. The subjects were instructed to keep the tip of the arrow as close as possible to the red cross for 10 s. There were 32 conditions (4 force levels × 8 directions), each was repeated twice. The conditions were presented in a random order. In total, 512 trials were analyzed (8 instructed directions × 4 targeted force magnitudes × 8 subjects).

Data Collection and Analysis

The force signals were amplified (Kistler model 5010) and digitized using a 16-bit A/D converter (PCI-6225, National Instruments, Austin, TX) at 1000 Hz. The data were collected using a custom program written in LabVIEW (National Instruments). The data analysis was performed using a custom program written in Matlab (The MathWorks, Natick, MA).

The first 4 s of each trial, while the subject was reaching the prescribed force level, and stabilizing their performance, were discarded. For the remaining 6 s of data, the forces were smoothed using a sixth-order Butterworth low-pass filter at 20 Hz. All further analysis on the forces was performed after first dividing by the MVC for that direction.

By measuring the lengths of the limb segments, and their orientations, we constructed the Jacobian of the system:

$$J(\theta_1 = 0, \theta_2 = 90°) = \begin{bmatrix} -l_2 & -l_2 \\ l_1 & 0 \end{bmatrix} \quad (1)$$

where l_1 and l_2 are the lengths of the upper arm, and the distance from the elbow to the handle, respectively, and θ_1 and θ_2 are the angles of the shoulder and elbow joints, respectively, as shown in Figure 1A. Using the Jacobian (Equation 1), we estimated the joint torques used to produce the observed force:

$$\mathbf{T} = J^T \mathbf{F} = \begin{bmatrix} -l_2 & l_1 \\ -l_2 & 0 \end{bmatrix} \begin{bmatrix} F_x \\ F_y \end{bmatrix} \quad (2)$$

where $\mathbf{T}$ is the vector of joint torques and $\mathbf{F}$ is the vector of endpoint force components (see Zatsiorsky, 2002), made up of the left–right (F_x) and forward–back (F_y) components. The joint torques were calculated by employing Equation 2, using the normalized forces.

Spectral Analysis

Spectral analysis was performed on the magnitude of the force using Welch's periodogram method, with a window size of 64, after resampling the force to 100 Hz. This led to 0.0396 Hz frequency bins. The mean power (averaged across subjects, by force level) was plotted as a function of the frequency, additionally the sum of the power in the bins 0–4 Hz, 4–8 Hz, and 8–12 Hz was presented, as these ranges represent specific neurophysiological processes. Sensorimotor processes should be mostly in the 0–4 Hz range, whereas tremor and signal dependent noise should be in the higher ranges (Vaillancourt & Newell, 2003).

Variance

The variance of the force was calculated for each trial using the force data sampled every 100 ms (i.e., 60 samples from 6 s). From the two repetitions performed for each condition, the one with the lowest mean (over F_x and F_y) of the variance was selected. This was done to minimize the chance of using trials in which subjects had difficulty performing the task. The magnitude of the force vector ($|F|$) and forces perpendicular to the average produced direction $F_\perp$, calculated by projecting the force onto a vector perpendicular to the average direction of force production, were computed. The instantaneous angles of force production were also calculated, using

$$\theta = \arctan\left(\frac{F_y}{F_x}\right). \quad (3)$$

where $|F|$ and θ describe the force vector in polar coordinates. Angles were converted to degrees throughout the results to aid in interpretation.

Calculation of average across-subjects standard deviations was performed by calculating the variances of the corresponding quantities for each subject, taking the group mean, and then taking the square root. The standard error s of the standard deviation is calculated by (Ahn & Fessler, 2003):

$$s \approx \frac{1}{\sqrt{2(n-1)}}\sigma \quad (4)$$

where n is the number of subjects and σ is the standard deviation. Means and standard deviations of angles were calculated using circular statistics (Berens, 2009).

Statistical Analysis

Linear regression of standard deviations of $|F|$ and $F_\perp$ on the targeted force magnitudes F_i (in percentage of the MVC) were computed. For the force angle, regression was performed on the equation $SD(\theta) = a + b \times 1/F_i$, where a and b are the regression coefficients and F_i is the instructed force magnitude. Repeated measures analyses of variance (ANOVAs) were performed on the regression coefficients,

with the factor direction (4 directions; opposite directions were combined). Paired t tests were used to compare the slopes of $|F|$ and $F_\perp$.
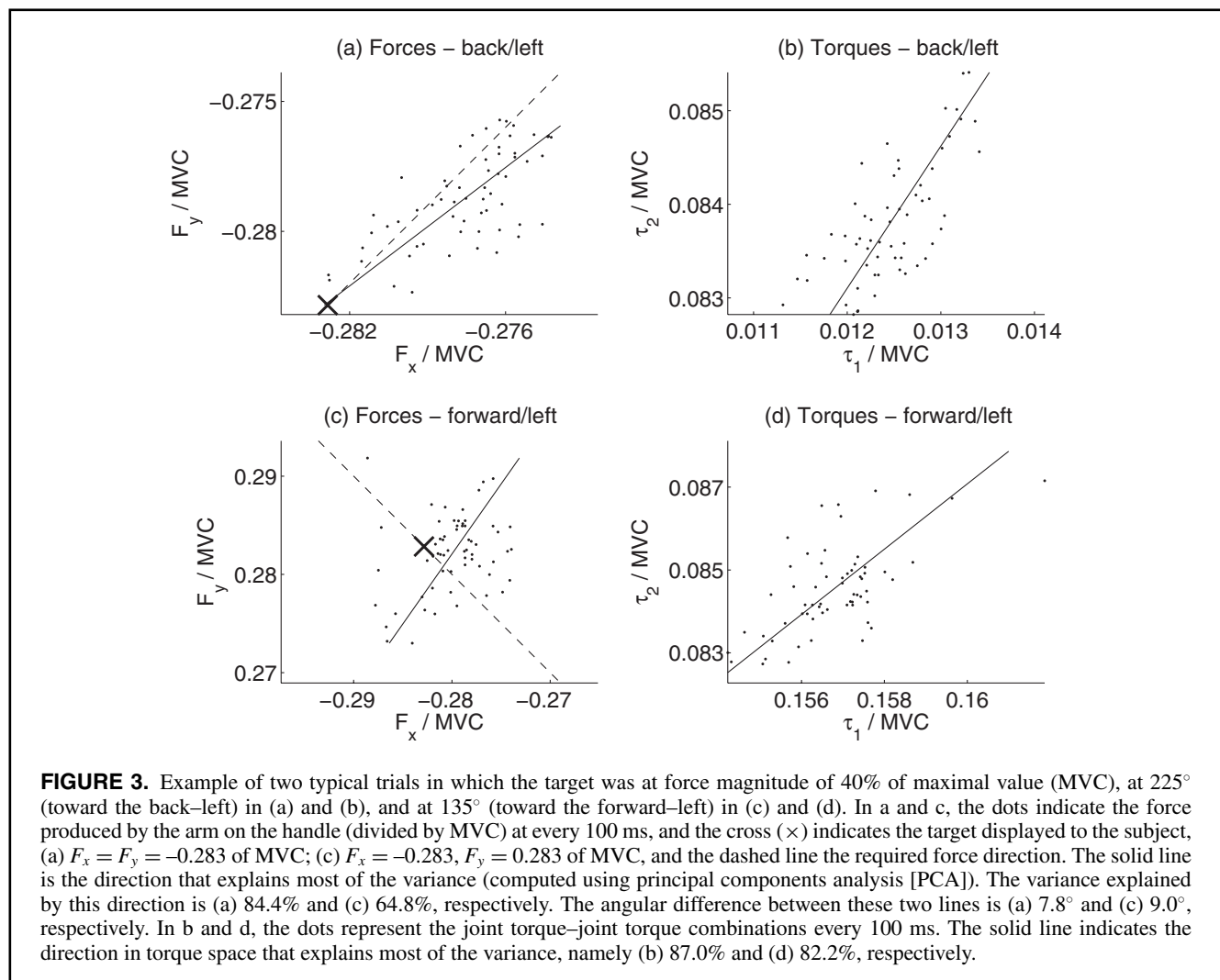
Statistical analysis of the joint torques τ_1 and τ_2 included computation of the regression of the torque variability (standard deviations) on the torque magnitude (i.e., $|\tau_1|$ and $|\tau_2|$). Two-way repeated measures ANOVAs were performed to determine the effect of the endpoint force magnitude and direction on the τ_1 and τ_2 standard deviation. The statistical analysis was performed using SPSS 17.0 (IBM, Chicago, IL), and the significance level was set at 0.05.
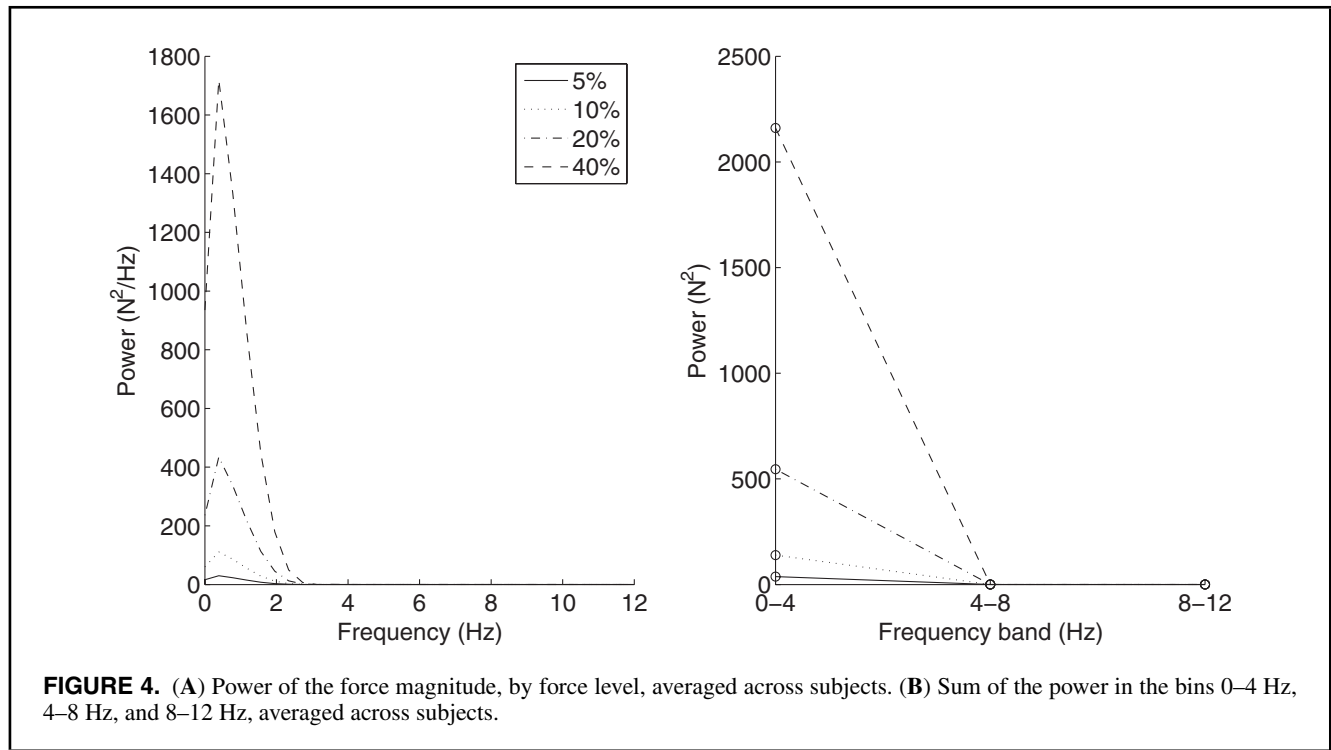
Principal components analysis (PCA) was performed using Matlab in force ($F_x - F_y$) and torque ($\tau_1 - \tau_2$) spaces on the decimated data (i.e., at every 100 ms, as was used for the variance calculations) for each trial. The direction of the first principal component was computed, that is, the direction along which the projection of the points (after subtracting the mean) describes the greatest amount of variance. Additionally, the amount of variance explained by the first component

was computed. Only trials in which the amount of variance explained by the first component was greater than 80% are included in the histograms presented. In a 2-D space the PCA results may be analogous to the computation of simple linear correlation. However, we prefer using the PCA because its results do not depend on the orientation of the reference axes. When the data are mainly spread along a coordinate axis, the coefficient of correlation could be zero, which is not very informative, whereas in the PCA the data distribution along the principal component axes (i.e., the amount of total variance explained by the individual principal components) can still be determined.

Results

After a short period of familiarization, all the subjects were able to successfully complete the task. Two typical trials are shown in Figure 3.

FIGURE 3. Example of two typical trials in which the target was at force magnitude of 40% of maximal value (MVC), at 225° (toward the back–left) in (a) and (b), and at 135° (toward the forward–left) in (c) and (d). In a and c, the dots indicate the force produced by the arm on the handle (divided by MVC) at every 100 ms, and the cross ($\times$) indicates the target displayed to the subject, (a) $F_x = F_y = -0.283$ of MVC; (c) $F_x = -0.283$, $F_y = 0.283$ of MVC, and the dashed line the required force direction. The solid line is the direction that explains most of the variance (computed using principal components analysis [PCA]). The variance explained by this direction is (a) 84.4% and (c) 64.8%, respectively. The angular difference between these two lines is (a) 7.8° and (c) 9.0°, respectively. In b and d, the dots represent the joint torque–joint torque combinations every 100 ms. The solid line indicates the direction in torque space that explains most of the variance, namely (b) 87.0% and (d) 82.2%, respectively.

FIGURE 4. (**A**) Power of the force magnitude, by force level, averaged across subjects. (**B**) Sum of the power in the bins 0–4 Hz, 4–8 Hz, and 8–12 Hz, averaged across subjects.
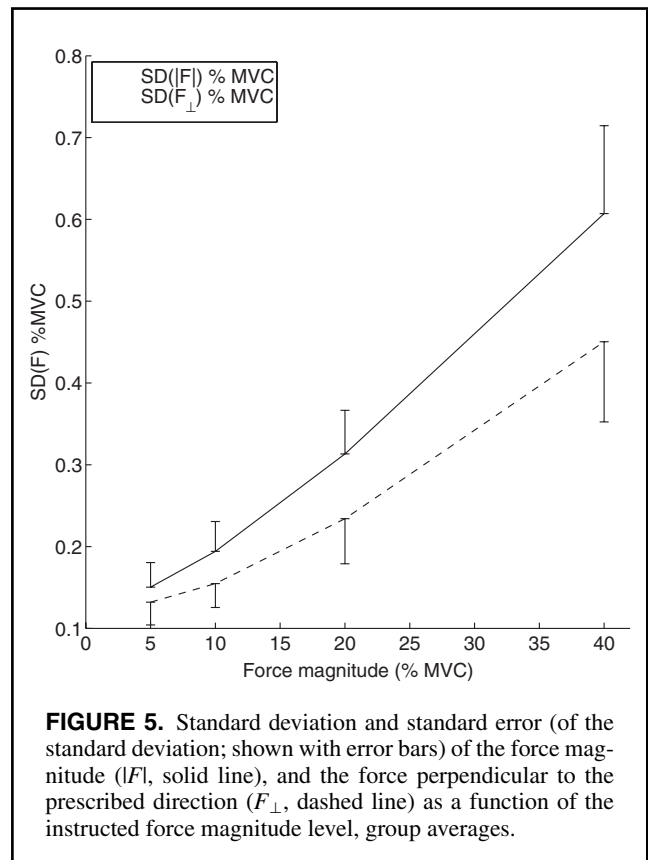
Spectral Analysis

The results of the spectral analysis, averaged across subjects, are shown in Figure 4. Almost all the power, for all subjects, was located within the 0–4 Hz band. The power increased as the prescribed force level increased. Hence the data agree only in part with the concept of the signal-dependent noise: the power increased with the force level but the peak power was observed at the much lower rate (0–4 Hz band) than it was expected from the literature (Jones et al., 2002). This range indicates that the observed variation was mostly due to slow sensorimotor processing.

Standard Deviation of the Forces and Angle of Force Production

The standard deviations of the forces were calculated for each trial and averaged across the targeted force magnitudes, directions, and subjects. In all calculations regarding mean standard deviations, the calculation was performed by taking the square root of the mean variance. When considered as a function of the targeted force magnitude, the standard deviation of the force magnitude increased approximately linearly with the increase in the targeted force magnitude, as expected (Hypothesis 1). The standard deviations, averaged across directions and subjects for each targeted force level, are shown in Figure 5.

The mean slope of the relation standard deviation of |F| versus instructed force magnitude F_i, % of MVC, averaged across subjects, was 0.013 (±0.003), whereas the mean in-

FIGURE 5. Standard deviation and standard error (of the standard deviation; shown with error bars) of the force magnitude (|F|, solid line), and the force perpendicular to the prescribed direction ($F_\perp$, dashed line) as a function of the instructed force magnitude level, group averages.

tercept of the same relationship was 0.057 ($\pm$0.020). The median R^2 value of the fit was .94 (range = .74–.95).

The standard deviation of the force perpendicular to the average produced direction also increased approximately linearly with the increase in targeted force magnitude (Hypothesis 2), although the magnitude of the slope was smaller. The standard deviations of $F_\perp$, averaged across subjects and conditions, are also shown in Figure 5. The slope of this relation, averaged across subjects, was 0.008 ($\pm$0.004), whereas the average intercept was 0.060 ($\pm$0.025). The median R^2 value of the fit was .90 (range = .67–.94). A paired t test, comparing the slopes of $|F|$ and $F_\perp$, found that the slope for $|F|$ was significantly greater than that for $F_\perp$ ($p < .0001$).

To determine whether the slope of the $SD(|F|)$ versus targeted force magnitude relation was dependent on the direction, an ANOVA was performed on the slope, with factor direction. A main effect of direction, $F(3, 31) = 4.38$, $p < .05$, was found. A Tukey post hoc test showed that the slopes for the 135°/315° angles ($M = 0.016$, $SD = 0.007$) were significantly greater than the slopes for the 90°/270° angles ($M = 0.010$, $SD = 0.004$) at the 0.05 level. The differences in other angle combinations were not significantly different. A similar ANOVA performed on the slope of $SD(F_\perp)$ found a main effect of direction, $F(3, 31) = 7.75$, $p < .01$. A Tukey post hoc test showed that the slopes for 0°/180° ($M = 0.010$, $SD = 0.004$), and for 135°/315° ($M = 0.013$, $SD = 0.008$) were significantly greater than the slopes for the other two directions: 90°/270° ($M = 0.0043$, $SD = 0.0025$) and 45°/225° ($M = 0.0047$, $SD = 0.0029$).

In contrast to the force magnitude variability, and in contrast to our expectations (see the Hypothesis 3), the standard deviation of the force angle decreased as the force magnitude increased. This is illustrated in Figure 6. Due to the shape of the relation, regression was performed on the equation $SD(\theta) = a + b \times 1/F_i$, where a and b are the coefficients that are fit, and F_i is the instructed force level. The average value of b was 0.072 ($\pm$0.033), and the median R^2 for the fit was .62 (range = .54–.81). An ANOVA performed on the value of b with the factor direction showed a significant main effect, $F(3, 31) = 3.63$, $p < .05$. A Tukey post hoc test showed that the slope for the 90°/270° direction ($M = 0.043$, $SD = 0.034$) was significantly smaller that the slope for the 0°/180° direction ($M = 0.105$, $SD = 0.083$). The other directions were not significantly different from each other.
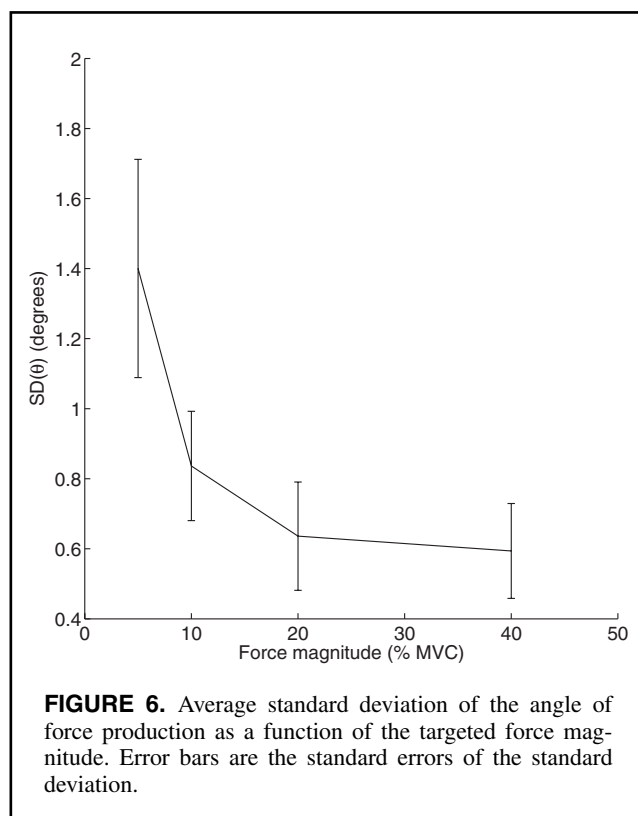
To further explore the effect of direction on the variability of the angle of force production, the mean standard deviation across subjects is plotted in Figure 7. Three directions had relatively low standard deviations: 90° ($M = 0.56°$), 270° ($M = 0.52°$), and 225° ($M = 0.58°$). Two directions had relatively high standard deviations: 0° ($M = 1.33°$) and 315° ($M = 1.21°$). In the remaining three directions the angular variability was average, neither maximal nor minimal.
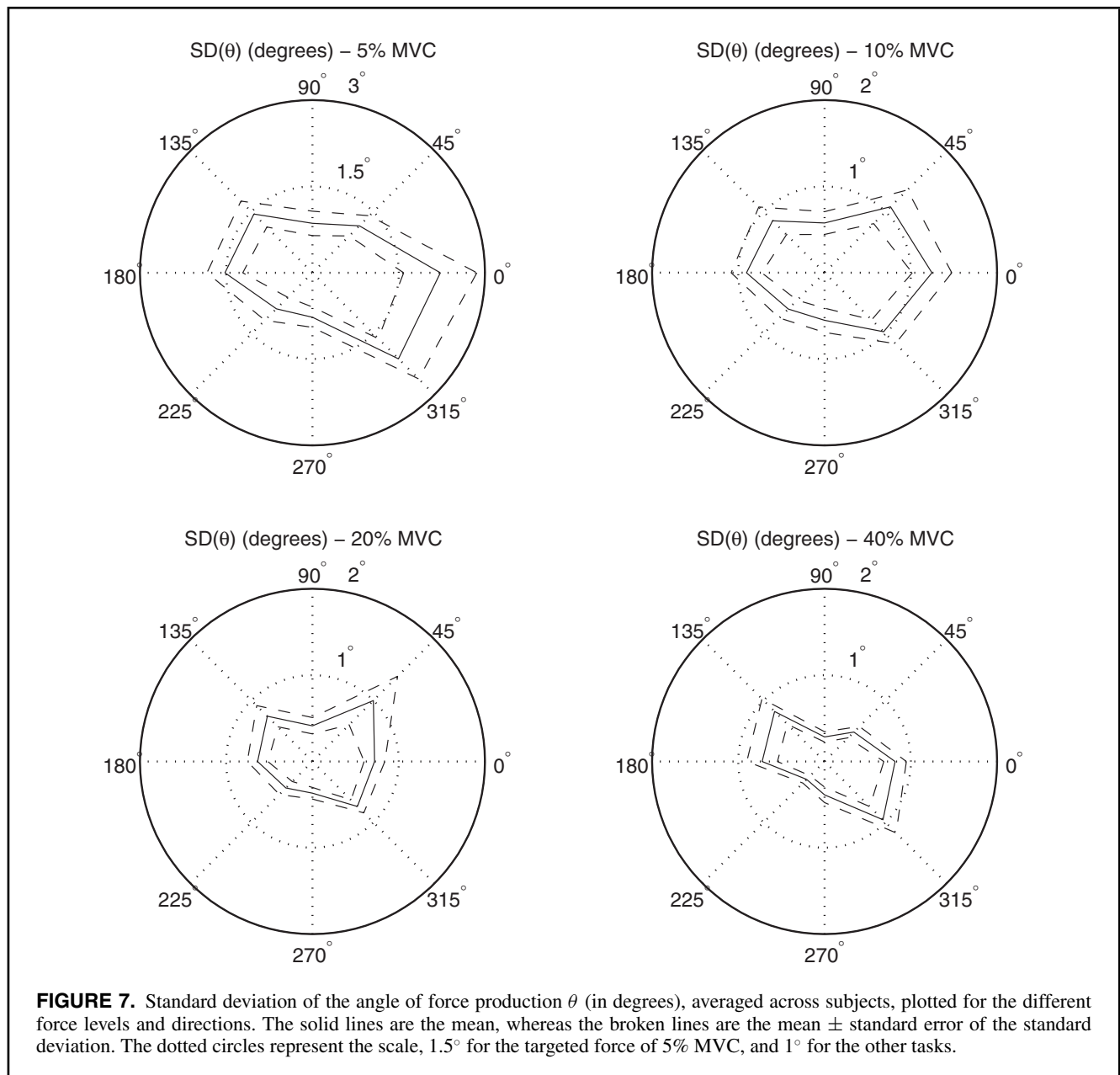
Major Axes of the Force Distribution

In the PCA we were mainly interested in the direction of the first principal component, whether the force–force distribution ellipse was well aligned with the targeted force direction (Hypothesis 4). Histograms of the direction of the first principal component that fall within the shown quadrant (when the variance accounted for by the first component was greater than 80%) are shown in endpoint force space in Figure 8. When a large number of the directions of the first principal component fall into one histogram bin, this means that for many of the trials the variance was distributed close to this direction. In this space (of endpoint force), the major axes of the force distribution were well aligned with the angle of force direction in some directions but not in other. In particular, in the forward and backward directions (90° and 270°), as well as in diagonally forward–right (45°) and backward–left (225°) directions of force production, the average differences ($\Delta\theta$) between the direction of the first principal component and the instructed force direction were all below 10.7°. That is, the variance in endpoint force was mostly distributed along the direction of force production. In the other four directions, the variance explained by the first principal component was less than 80% in most of the cases (183 cases out of 256), indicating a relatively low correlation of the F_x and F_y values.

Joint Torque Variability

The joint torques were computed using the Jacobian, as described in Equation 2. The means and standard deviations

FIGURE 6. Average standard deviation of the angle of force production as a function of the targeted force magnitude. Error bars are the standard errors of the standard deviation.

FIGURE 7. Standard deviation of the angle of force production θ (in degrees), averaged across subjects, plotted for the different force levels and directions. The solid lines are the mean, whereas the broken lines are the mean $\pm$ standard error of the standard deviation. The dotted circles represent the scale, $1.5°$ for the targeted force of 5% MVC, and $1°$ for the other tasks.

of the joint torques can be found in Table 1. As designed, these values confirmed the predictions regarding which torques would be close to zero (see legend of Figure 1).

We first considered the variability (standard deviation) of the individual joint torques and then the concurrent changes of the torques at the two joints.

The effect of joint torque magnitude on torque variability (Hypothesis 5) was explored by performing a regression, with the equation $SD(\tau_i) = a \times |\tau_i| + c$. The average value of a was 4.07 (± 1.82) $\times 10^{-4}$ for τ_1 and 2.96 (± 1.12) $\times 10^{-4}$ for τ_2. The average values of the intercept were 0.012 (± 0.003) m^{-1} for τ_1 and 0.011 (± 0.003) m^{-1} for τ_2. The average R^2 values for the fits were .64 (± 0.28) and .68

($\pm.07$), respectively. All correlations were significant at the .05 level.

Correlations between the standard deviation at a given joint and torque magnitude at another joint were also computed. The correlations were calculated for each subject over all conditions and then averaged across subjects, using the Fisher transform (Silver & Dunlap, 1987). The correlations were low. The average correlations were 0.39 (± 0.24) for the standard deviation of τ_2 versus $|\tau_1|$ correlation and 0.34 (± 0.21) for the standard deviation of τ_1 versus $|\tau_2|$ correlation, respectively. These correlations were not significant ($p > .05$) for 6 of the 8 subjects for $SD(2)$ and τ_1, and for 4 of the 8 subjects for $SD(1)$ and τ_2.
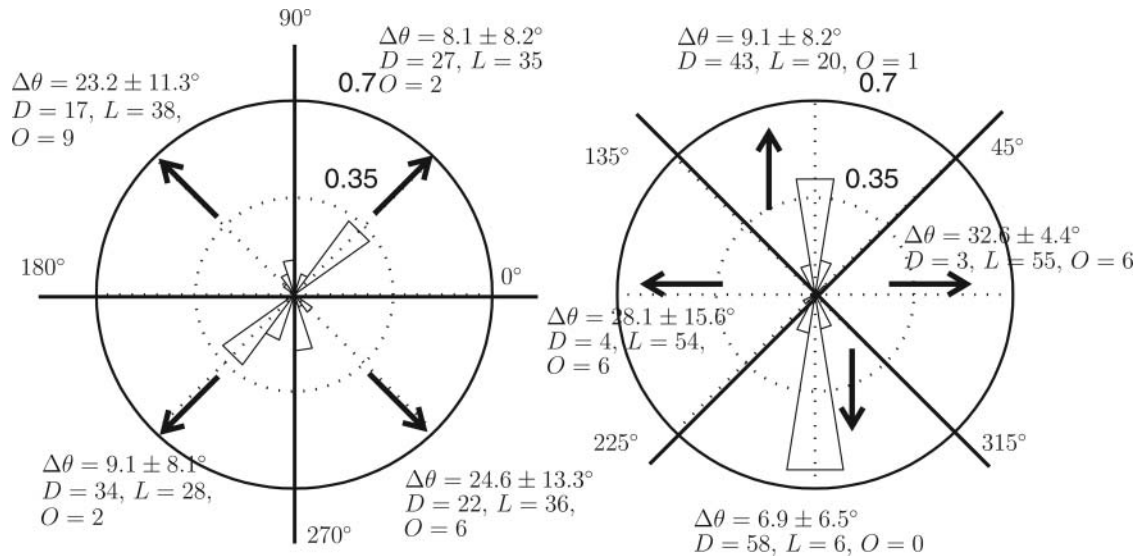
FIGURE 8. Angle histogram of the directions of the major PCA axes in force space. In each quadrant, the frequencies of the directions of the major PCA axes that fell within that quadrant are shown (total number shown on the histogram in each direction as D), divided into 5 equal sized bins of 18°. Not included in the histograms are those in which the variance explained by the first principal component was less that 80% (shown as L), and those where the axes fell in another quadrant (shown as O), $D + L + O = 64$. Because each major axis falls in two quadrants (i.e., the opposite quadrants, such as top right and bottom left), the histogram is shown in the quadrant corresponding to the direction of force production for clarity. The arrows on the graph indicate the direction of required force production. The histograms are normalized such that one indicates all trials for a given direction. The mean and standard deviation of the difference ($\Delta\theta$) between the direction of the axis of the first principal component and the instructed force direction are indicated.

The partial correlations between the standard deviation of τ_1 and that of τ_2 controlling for $|\tau_1|$ and $|\tau_2|$ were calculated for each subject over all conditions, then averaged across subjects, using the Fischer transform. The average values of the partial correlations, with the effects of τ_1 and τ_2 removed, were 0.64 (±0.28) and 0.68 (±0.30), respectively. Both partial correlations were significant for all subjects at the .05 level.

With regard to the torque–torque concomitant changes in the individual trials, when viewed in torque space, the variance explained by the first principal components was greater than 80% in most of the trials (390 out of 512). The variance explained by the first component was significantly larger in torque space compared to force space (paired t test, $p < .0001$), and nearly always (386 out of 390) fell in the first quadrant (i.e., positive correlation between the joint torques), as shown in Figure 9.

The direction of the first principal axes in the torque–torque space depended on the targeted direction of the endpoint force. This fact is confirmed by an ANOVA with factor direction (8 levels), $F(7, 382) = 16.94, p < .001$. The direction of the axes of the first principal component did not correspond to the direction of concomitant torque–torque variation assuming only the force magnitude varies. For example, for force production to the right, the angle in torque–torque space corresponding to such force magnitude variation is

135°, whereas the angle of the first principal component was on average 36.2° ($\pm0.17°$).

Discussion

We discuss first the data obtained in the force space, in particular whether the formulated hypotheses were confirmed or compromised, and then the data obtained in the torque space.

The first hypothesis was confirmed, agreeing with findings from previous studies (Hamilton et al., 2004; Schmidt et al., 1979): the standard deviation of the force along the average direction of force production, $|F|$, was linearly related to the magnitude of the force. The small but nonzero intercept observed (see Figure 5) may be the result of two processes occurring in parallel—in addition to the task of force production, the subjects also visually perceived the force level by looking at the monitor. As the feedback scale was the same for all levels of force production, this error is expected to be approximately constant across force levels, and may explain the nonzero intercept (Smeets & Brenner, 2008). It should be noted that if rather than plotting the standard deviation of force magnitude $SD(|F|)$, we instead divided it by the mean force magnitude (i.e., compute the coefficient of variation [CV]), we would also get a decrease in the CV as force magnitude increases, as was found previously (Hamilton et al.;

J. Friedman, M. L. Latash, & V. M. Zatsiorsky

TABLE 1. Mean and Standard Deviations (Across Subjects) of the Joint Torques Calculated Using Equation (2). All Values are Divided by the MVC for that Direction, and Multiplied by 100.

Direction		5% MVC	10% MVC	20% MVC	40% MVC
0°	τ_1	-1.692 (±0.170)	−3.257 (±0.207)	−6.395 (±0.371)	−12.751 (±0.816)
	τ_2	−1.683 (±0.155)	−3.238 (±0.202)	−6.379 (±0.353)	−12.713 (±0.776)
45°	τ_1	−0.163 (±0.119)	−0.315 (±0.202)	−0.524 (±0.368)	−1.111 (±0.696)
	τ_2	−1.148 (±0.102)	−2.250 (±0.171)	−4.456 (±0.296)	−8.972 (±0.592)
90°	τ_1	1.451 (±0.091)	2.865 (±0.200)	5.597 (±0.321)	11.166 (±0.581)
	τ_2	−0.002 (±0.034)	−0.009 (±0.030)	0.001 (±0.028)	−0.012 (±0.028)
135°	τ_1	2.226 (±0.227)	4.358 (±0.362)	8.661 (±0.715)	17.286 (±1.540)
	τ_2	1.200 (±0.110)	2.340 (±0.209)	4.624 (±0.417)	9.202 (±0.872)
180°	τ_1	1.641 (±0.154)	3.224 (±0.245)	6.434 (±0.381)	12.785 (±0.792)
	τ_2	1.644 (±0.149)	3.235 (±0.259)	6.415 (±0.388)	12.757 (±0.818)
225°	τ_1	0.156 (±0.126)	0.264 (±0.171)	0.554 (±0.374)	1.101 (±0.722)
	τ_2	1.224 (±0.161)	2.286 (±0.184)	4.516 (±0.309)	8.995 (±0.594)
270°	τ_1	−1.462 (±0.124)	−2.864 (±0.168)	−5.641 (±0.333)	−11.138 (±0.574)
	τ_2	0.024 (±0.047)	0.008 (±0.034)	−0.006 (±0.023)	0.002 (±0.024)
315°	τ_1	−2.216 (±0.187)	−4.300 (±0.181)	−8.512 (±0.443)	−16.934 (±0.699)
	τ_2	−1.189 (±0.109)	−2.289 (±0.146)	−4.543 (±0.333)	−9.041 (±0.580)

Mintz & Notterman, 1965; Moritz, Barry, Pascoe, & Enoka, 2005).

The second hypothesis was also confirmed: the standard deviation of the force perpendicular to the average direction of force production $F_\perp$ was also proportional to force magnitude.

The third hypothesis was found to be false. The standard deviation of the angle of force production θ, in contrast, decreased with increasing force magnitude. This means that to produce higher angular precision, higher absolute force should be used. The standard deviation of the angle is approximately linearly related to the standard deviation of $F_\perp$ divided by $|F|$. As the standard deviation of $F_\perp$ increases at a lower rate than the standard deviation of force magnitude $|F|$, this causes the reduction in the standard deviation of the angle (or increase in precision) with increasing forces. This finding is not merely due to the constant gain of visual feedback: a further study (Xu, Latash, & Zatsiorsky, in preparation) using the same apparatus but in which the visual feedback was scaled according to the target force magnitude did not find a systematic increase in angular variability with the increase of the prescribed force magnitude. Although changing the form of visual feedback may change the amount of variability (Tracy, 2007), it is unlikely to change the relative amounts of variability observed in the directions parallel and perpendicular to the instructed direction of force production, which explains our observation about the variation in angle of force production.

The variability did vary across directions: In the directions of 90° and 270° (corresponding to the directions in which $\tau_2 = 0$; see Table 1) and 225° (corresponding to the direction in which τ_1 is close to zero; see Table 1), the standard deviation was relatively low, whereas it was higher in the 0°

and 315° directions, corresponding to approximately equal torque magnitudes from the elbow and shoulder.

The fourth hypothesis, that the axes of the principal components of the force–force distributions would be aligned with the $|F|$ and $F_\perp$ directions, was accepted only for some directions of force production. In the $F_x - F_y$ space, the principal component axes were well aligned with the direction of force production for force production in the forward (90°) and backward (270°) directions as well as in diagonally forward–right (45°) and backward–left (225°) directions. This corresponds to directions in which the expected joint torque for the elbow is zero (forward–back) and for the shoulder is close to zero (diagonal forward–right and backward–left). Hence, in the previous directions the data support the fourth hypothesis: the data are distributed mainly along the instructed force direction. In the other directions (left–right, diagonally forward–left and backward–right), the first principal component only accounted for more than 80% of the variance in a small proportion of the cases.

Considering the task in the force space, two possible outcomes can be expected. In particular, if the two quantities (e.g., $|F|$ and $F_\perp$) are specified without covariation, then performing PCA on the data should find that the axis that describes most of the variation (major axis) should correspond to either the $|F|$ or $F_\perp$ direction, assuming unequal variance along the two axes. If the amount of variation were the same along the two axes (such that the data points would be distributed approximately in a filled circle), then while the major axis of the distribution could be in any direction, the variance explained by the first PC would be relatively low (i.e., about 50%). For four of the directions (90°, 270°, 45°, and 225°—in these tasks, as it was mentioned previously, the torque at one of the joints was either zero or close to zero),
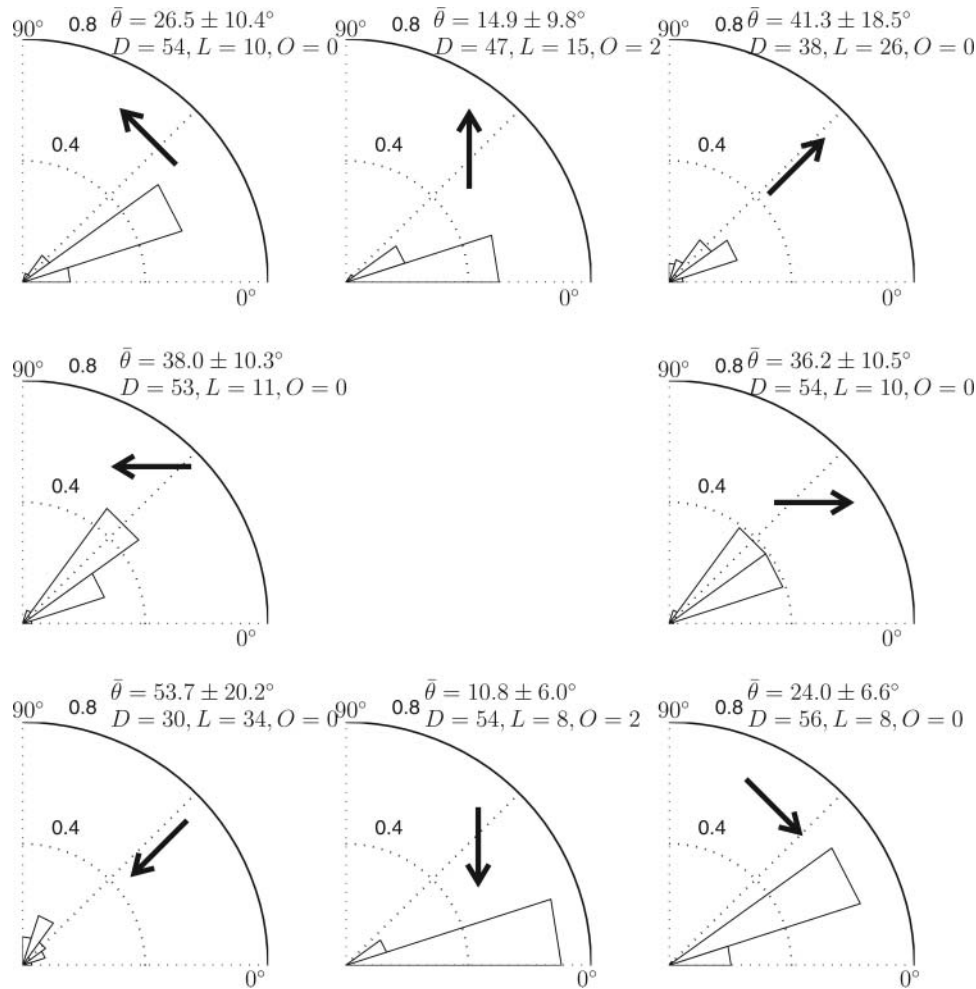
FIGURE 9. Angle histogram for the major PCA axes in torque space. The procedure similar to one used in Figure 8 is used. The arrows indicate the targeted force directions in the force space. In 122 (out of 512) cases, the variance explained by the first principal component was less than 80% (shown as L). In the rest of the cases, most (386 out of 390) were in the range $0°$ to $90°$ (shown as D), the other four cases are shown as O. The mean angle of the direction of the first PCA axis $\bar{\theta}$ is indicated for each endpoint force direction. The $0°$ direction corresponds to the direction of the first PCA axis along the t_1 axis; $90°$ is the direction along the t_2 axis. The concentric circles (marked with 0.4 and 0.8) indicate the relative frequency (1 = all trials for this condition).

the distribution of directions of the PC axes corresponded to the first case (most of the variance was along the $|F|$ axis), whereas in the other four the low amount of variance explained by the first PC is consistent with the second case (approximately equal variation along the $|F|$ and $F_\perp$ directions). Both of these findings are consistent with the notion that for this task force production is controlled without substantial covariation of force magnitudes along the direction of force production, and the perpendicular direction. This seems to contradict the previous finding that the standard deviations of $|F|$ and $F_\perp$ increase linearly with force rate, albeit at different rates. However, even if both do increase in a linear fashion, this does not necessarily imply that they are coordinated, and the results of the PCA suggest that they are not for this task.

As the endpoint force is a result of mechanical transformation of the joint torques, analysis of the torque–torque variations can be useful. Some of the facts on the torque magnitude are a trivial consequence of the mechanical relations described by Equation 2. For example, it is evident than the force magnitude depends on the torque magnitude. Hence comparing the torque magnitudes across the trials with different force magnitude is not very informative. However, data on the torque variability are far from trivial. They can open a window for understanding the origin of the variability, such as whether the variability is due to the neuromotor noise at the low levels of the control hierarchy (e.g., individual muscles, motoneuron pools) or the variability of the common drive to the muscles serving the two joints.

Similar to the previous findings, the fifth hypothesis, that the joint torque variability would increase with the torque magnitude, was also confirmed. In addition, the following facts on the torque variability reported previously attract attention: (a) the torque–torque correlations in the trials were mainly positive (Figure 9; i.e., a torque increase [decrease] at one joint was mainly associated with similar changes of the torque at the other joint); (b) across the trials there were no significant correlation between the torque standard deviation at one joint and the torque magnitude at the other joint (the correlation between the torque magnitude and its variability was statistically significant, as should be expected); and (c) when the effects of the torque magnitude were eliminated, the partial correlations between the standard deviations at the two joints were statistically significant. These facts, especially a and c, lend support for the hypothesis that the torque variations are mainly due to the variability of the central common drive to muscles involved in the endpoint force production in the targeted direction (and not, for example, due to the peripheral noise at the level of individual muscles; see also Jones et al., 2002; van Beers, Haggard, & Wolpert, 2004). The spectral analysis, which showed most of the power was found in the range of 0–4 Hz, instead of higher frequencies (Jones et al.), suggested that these variations are likely not due to signal-dependent noise but rather variations in the specification of the endpoint force. Still there exists an option that the differences in the frequencies could be due to the different mechanical properties of the studied objects: in Jones et al.'s study, in which the idea of the central origin of the signal dependence noise was experimentally confirmed, they recorded static forces exerted by the distal phalanx of the thumb, whereas in our study the arm force was recorded. It is possible that due to mechanical properties of the arm, such as large inertia and damping, the high-frequency components of the muscle force oscillations were not transmitted to the palm and the arm essentially worked as a low-frequency pass filter. The mechanical vibrations at the higher frequencies and acceleration levels are absorbed by the hand and arm to a larger degree than low-frequency vibrations (Burström & Bylund, 2000).

Although the obtained data agree with the hypothesis that torque variations are mainly due to the variability of the central common drive to the muscles, the present research is not sufficient to prove it. In particular, the research does not address the possible contribution of the two-joint muscles serving the shoulder and elbow joints (the long head of the biceps brachii, which is a flexor at both joints of interest, and the long head of triceps, which is an elbow extensor and at the shoulder joint, assists in upper arm retroversion [i.e., moving the arm backward, toward the back of the body]). At the body position used in the present study, increased neural drive to these muscle heads may induce unidirectional (flexion–extension) changes at the both joint torques. However, the moment arms of these muscle heads at the shoulder joint are small and their contribution to the torque production

is limited (Pigeon, Yahia, & Feldman, 1996). Unfortunately, we did not include in the research the tasks where the endpoint force is exerted due to the joint torques in the opposite directions (i.e., the tasks with the EF (shoulder extension, elbow flexion) and FE (shoulder flexion, elbow extension) torques). We consider this is a limitation of the present study.

It is interesting to compare the obtained results with the data on the joint–segment tremor when subjects were asked to maintain an extended arm posture. Studying such a posture, Morrison and Newell (2000) concluded that the intralimb segment correlations were characterized by compensatory (out of phase) coupling between the upper arm–forearm and hand–index finger segment pairs of each limb. On appearance, our data contradict this finding (we found mainly positive, that is, in-phase correlations). However, Morrison and Newell studied kinematic tasks (the limbs' acceleration was recorded), whereas we studied static tasks (the forces were recorded). In the present research, the task was not redundant (two joint torques define two endpoint force components in a unique way). If tasks with a larger number of joints were investigated (e.g., if the finger movements were considered or the forces were exerted by a fingertip) the task would become redundant in kinematics, but it would become overdetermined in statics (the redundancy vs. overdeterminacy issue is discussed in Zatsiorsky, 2002). To our knowledge, overdetermined static tasks have not been studied so far. Hence, the kinematic and static tasks may require different control mechanisms. It seems that the difference between the data of Morrison and Newell and the present findings is due to the difference in the control of kinematics and statics tasks.

On the whole, coordinated changes in both joint torques suggest that the torque variability was due to the variability of the common drive to the muscles serving two joints and not, for example, to the noise at the level of individual muscles or motoneuron pools.

REFERENCES

Ahn, S., & Fessler, J. A. (2003). *Standard errors of mean, variance, and standard deviation estimators*. Technical Report, Comm. and Sign. Proc. Lab, EECS Department, University of Michigan, Ann Arbor, Michigan. Retrieved from http://www.eecs.umich.edu/~fessler/papers/files/tr/stderr.pdf

Berens, P. (2009). CircStat: A MATLAB toolbox for circular statistics. *Journal of Statistical Software*, *31*(10), 1–21.

Burström, L., & Bylund, S. H. (2000). Relationship between vibration dose and the absorption of mechanical power in the hand. *Scandinavian Journal of Work, Environment & Health*, *26*(1), 32–36.

Carlton, L. G., & Newell, K. M. (1993). Force variability and characteristics of force production. In K. M. Newell & D. M. Corcos (Eds.), *Variability and motor control* (pp. 15–36). Champaign, IL: Human Kinetics.

Gao, F., Latash, M., & Zatsiorsky, V. (2005). Control of finger force direction in the flexion-extension plane. *Experimental Brain Research*, *161*, 307–315. doi:10.1007/s00221-004–2074-z

Hamilton, A., Jones, K., & Wolpert, D. (2004). The scaling of motor noise with muscle strength and motor unit number in humans. *Experimental Brain Research*, *157*, 417–430.

Harris, C. M., & Wolpert, D. M. (1998). Signal-dependent noise determines motor planning. *Nature*, *394*, 780–784. doi:10.1038/29528

Hong, S. L., Lee, M.-H., & Newell, K. M. (2007). Magnitude and structure of isometric force variability: Mechanical and neurophysiological influences. *Motor Control*, *11*, 119–134.

Jones, K. E., Hamilton, A. F. de C., & Wolpert, D. M. (2002). Sources of signal-dependent noise during isometric force production. *Journal of Neurophysiology*, *88*, 1533–1544.

Kapur, S., Friedman, J., Zatsiorsky, V., & Latash, M. (2010). Finger interaction in a three-dimensional pressing task. *Experimental Brain Research*, *203*, 101–118. doi:10.1007/s00221-010–2213-7

Kutch, J. J., Kuo, A. D., Bloch, A. M., & Rymer, W. Z. (2008). Endpoint force fluctuations reveal flexible rather than synergistic patterns of muscle cooperation. *Journal of Neurophysiology*, *100*, 2455–2471. doi:10.1152/jn.90274.2008

Mintz, D. E., & Notterman, J. M. (1965). Force differentiation in human subjects. *Psychonomic Science*, *2*, 289–290.

Moritz, C. T., Barry, B. K., Pascoe, M. A., & Enoka, R. M. (2005). Discharge rate variability influences the variation in force fluctuations across the working range of a hand muscle. *Journal of Neurophysiology*, *93*, 2449–2459. doi:10.1152/jn.01122.2004

Morrison, S., & Newell, K. M. (2000). Limb stiffness and postural tremor in the arm. *Motor Control*, *4*, 293–315.

Newell, K. M., & Carlton, L. G. (1988). Force variability in isometric responses. *Journal of Experimental Psychology: Human Perception and Performance*, *14*(1), 37–44.

Newell, K. M., Deutsch, K. M., Sosnoff, J. J., & Mayer-Kress, G. (2006). Variability in motor output as noise. In K. Davids, S. Bennett, & K. M. Newell (Eds.), *Movement system variability* (pp. 3–24). Champaign, IL: Human Kinetics.

Pigeon, P., Yahia, L., & Feldman, A. G. (1996). Moment arms and lengths of human upper limb muscles as functions of joint angles. *Journal of Biomechanics*, *29*, 1365–1370. doi:10.1016/0021–9290(96)00031-0

Schmidt, R., Zelaznik, H., Hawkins, B., Frank, J., & Quinn, J. J. (1979). Motor-output variability: A theory for the accuracy of rapid motor acts. *Psychological Review*, *86*, 415–451.

Shapkova, E., Shapkova, A., Goodman, A., Zatsiorsky, V., & Latash, M. (2008). Do synergies decrease force variability? A study of single-finger and multi-finger force production. *Experimental Brain Research*, *188*, 411–425. doi:10.1007/s00221-008–1371-3

Sherwood, D., & Schmidt, R. (1980). The relationship between force and force variability in minimal and near-maximal static and dynamic contractions. *Journal of Motor Behavior*, *12*, 75–89.

Silver, N. C., & Dunlap, W. P. (1987). Averaging correlation coefficients: Should Fisher's z transformation be used? *Journal of Applied Psychology*, *72*, 146–148.

Slifkin, A. B., & Newell, K. M. (1999). Noise, information transmission, and force variability. *Journal of Experimental Psychology: Human Perception and Performance*, *25*, 837–851.

Slifkin, A. B., & Newell, K. M. (2000). Variability and noise in continuous force production. *Journal of Motor Behavior*, *32*, 141–50.

Smeets, J. B. J., & Brenner, E. (2008). Grasping Weber's law. *Current Biology*, *18*(23), R1089–R1090. doi:10.1016/j.cub.2008.10.008

Tracy, B. L. (2007). Visuomotor contribution to force variability in the plantarflexor and dorsiflexor muscles. *Human Movement Science*, *26*, 796–807. doi:10.1016/j.humov.2007.07.001

Tracy, B. L., Mehoudar, P. D., & Ortega, J. D. (2006). The amplitude of force variability is correlated in the knee extensor and elbow flexor muscles. *Experimental Brain Research*, *176*, 448–464. doi:10.1007/s00221-006–0631-3

Vaillancourt, D. E., & Newell, K. M. (2003). Aging and the time and frequency structure of force output variability. *Journal of Applied Physiology*, *94*, 903–912. doi:10.1152/japplphysiol.00166.2002

Valero-Cuevas, F. J., Venkadesan, M., & Todorov, E. (2009). Structured variability of muscle activations supports the minimal intervention principle of motor control. *Journal of Neurophysiology*, *102*, 59–68. doi:10.1152/jn.90324.2008

Van Beers, R. J., Haggard, P., & Wolpert, D. M. (2004). The role of execution noise in movement variability. *Journal of Neurophysiology*, *91*, 1050–1063.

Wing, A. M., & Kristofferson, A. (1973). Response delays and the timing of discrete motor responses. *Perception & Psychophysics*, *14*(1), 5–12.

Zatsiorsky, V. (2002). *Kinetics of human motion*. Champaign, IL: Human Kinetics.